Measurement of the $t\bar{t}$ Production Cross Section in $p\bar{p}$ Collisions at $\sqrt{s} = 1.96$ TeV

V. M. Abazov,[36] B. Abbott,[75] M. Abolins,[65] B. S. Acharya,[29] M. Adams,[51] T. Adams,[49] E. Aguilo,[6] S. H. Ahn,[31] M. Ahsan,[59] G. D. Alexeev,[36] G. Alkhazov,[40] A. Alton,[64,*] G. Alverson,[63] G. A. Alves,[2] M. Anastasoaie,[35] L. S. Ancu,[35] T. Andeen,[53] S. Anderson,[45] B. Andrieu,[17] M. S. Anzelc,[53] M. Aoki,[50] Y. Arnoud,[14] M. Arov,[60] M. Arthaud,[18] A. Askew,[49] B. Åsman,[41] A. C. S. Assis Jesus,[3] O. Atramentov,[49] C. Avila,[8] C. Ay,[24] F. Badaud,[13] A. Baden,[61] L. Bagby,[50] B. Baldin,[50] D. V. Bandurin,[59] P. Banerjee,[29] S. Banerjee,[29] E. Barberis,[63] A.-F. Barfuss,[15] P. Bargassa,[80] P. Baringer,[58] J. Barreto,[2] J. F. Bartlett,[50] U. Bassler,[18] D. Bauer,[43] S. Beale,[6] A. Bean,[58] M. Begalli,[3] M. Begel,[73] C. Belanger-Champagne,[41] L. Bellantoni,[50] A. Bellavance,[50] J. A. Benitez,[65] S. B. Beri,[27] G. Bernardi,[17] R. Bernhard,[23] I. Bertram,[42] M. Besançon,[18] R. Beuselinck,[43] V. A. Bezzubov,[39] P. C. Bhat,[50] V. Bhatnagar,[27] C. Biscarat,[20] G. Blazey,[52] F. Blekman,[43] S. Blessing,[49] D. Bloch,[19] K. Bloom,[67] A. Boehnlein,[50] D. Boline,[62] T. A. Bolton,[59] G. Borissov,[42] T. Bose,[77] A. Brandt,[78] R. Brock,[65] G. Brooijmans,[70] A. Bross,[50] D. Brown,[81] N. J. Buchanan,[49] D. Buchholz,[53] M. Buehler,[81] V. Buescher,[22] V. Bunichev,[38] S. Burdin,[42,†] S. Burke,[45] T. H. Burnett,[82] C. P. Buszello,[43] J. M. Butler,[62] P. Calfayan,[25] S. Calvet,[16] J. Cammin,[71] W. Carvalho,[3] B. C. K. Casey,[50] H. Castilla-Valdez,[33] S. Chakrabarti,[18] D. Chakraborty,[52] K. Chan,[6] K. M. Chan,[55] A. Chandra,[48] F. Charles,[19,**] E. Cheu,[45] F. Chevallier,[14] D. K. Cho,[62] S. Choi,[32] B. Choudhary,[28] L. Christofek,[77] T. Christoudias,[43] S. Cihangir,[50] D. Claes,[67] Y. Coadou,[6] M. Cooke,[80] W. E. Cooper,[50] M. Corcoran,[80] F. Couderc,[18] M.-C. Cousinou,[15] S. Crépé-Renaudin,[14] D. Cutts,[77] M. Ćwiok,[30] H. da Motta,[2] A. Das,[45] G. Davies,[43] K. De,[78] S. J. de Jong,[35] E. De La Cruz-Burelo,[64] C. De Oliveira Martins,[3] J. D. Degenhardt,[64] F. Déliot,[18] M. Demarteau,[50] R. Demina,[71] D. Denisov,[50] S. P. Denisov,[39] S. Desai,[50] H. T. Diehl,[50] M. Diesburg,[50] A. Dominguez,[67] H. Dong,[72] L. V. Dudko,[38] L. Duflot,[16] S. R. Dugad,[29] D. Duggan,[49] A. Duperrin,[15] J. Dyer,[65] A. Dyshkant,[52] M. Eads,[67] D. Edmunds,[65] J. Ellison,[48] V. D. Elvira,[50] Y. Enari,[77] S. Eno,[61] P. Ermolov,[38] H. Evans,[54] A. Evdokimov,[73] V. N. Evdokimov,[39] A. V. Ferapontov,[59] T. Ferbel,[71] F. Fiedler,[24] F. Filthaut,[35] W. Fisher,[50] H. E. Fisk,[50] M. Fortner,[52] H. Fox,[42] S. Fu,[50] S. Fuess,[50] T. Gadfort,[70] C. F. Galea,[35] E. Gallas,[50] C. Garcia,[71] A. Garcia-Bellido,[82] V. Gavrilov,[37] P. Gay,[13] W. Geist,[19] D. Gelé,[19] C. E. Gerber,[51] Y. Gershtein,[49] D. Gillberg,[6] G. Ginther,[71] N. Gollub,[41] B. Gómez,[8] A. Goussiou,[82] P. D. Grannis,[72] H. Greenlee,[50] Z. D. Greenwood,[60] E. M. Gregores,[4] G. Grenier,[20] Ph. Gris,[13] J.-F. Grivaz,[16] A. Grohsjean,[25] S. Grünendahl,[50] M. W. Grünewald,[30] F. Guo,[72] J. Guo,[72] G. Gutierrez,[50] P. Gutierrez,[75] A. Haas,[70] N. J. Hadley,[61] P. Haefner,[25] S. Hagopian,[49] J. Haley,[68] I. Hall,[65] R. E. Hall,[47] L. Han,[7] K. Harder,[44] A. Harel,[71] R. Harrington,[63] J. M. Hauptman,[57] R. Hauser,[65] J. Hays,[43] T. Hebbeker,[21] D. Hedin,[52] J. G. Hegeman,[34] J. M. Heinmiller,[51] A. P. Heinson,[48] U. Heintz,[62] C. Hensel,[58] K. Herner,[72] G. Hesketh,[63] M. D. Hildreth,[55] R. Hirosky,[81] J. D. Hobbs,[72] B. Hoeneisen,[12] H. Hoeth,[26] M. Hohlfeld,[22] S. J. Hong,[31] S. Hossain,[75] P. Houben,[34] Y. Hu,[72] Z. Hubacek,[10] V. Hynek,[9] I. Iashvili,[69] R. Illingworth,[50] A. S. Ito,[50] S. Jabeen,[62] M. Jaffré,[16] S. Jain,[75] K. Jakobs,[23] C. Jarvis,[61] R. Jesik,[43] K. Johns,[45] C. Johnson,[70] M. Johnson,[50] A. Jonckheere,[50] P. Jonsson,[43] A. Juste,[50] E. Kajfasz,[15] A. M. Kalinin,[36] J. M. Kalk,[60] S. Kappler,[21] D. Karmanov,[38] P. A. Kasper,[50] I. Katsanos,[70] D. Kau,[49] V. Kaushik,[78] R. Kehoe,[79] S. Kermiche,[15] N. Khalatyan,[50] A. Khanov,[76] A. Kharchilava,[69] Y. M. Kharzheev,[36] D. Khatidze,[70] T. J. Kim,[31] M. H. Kirby,[53] M. Kirsch,[21] B. Klima,[50] J. M. Kohli,[27] J.-P. Konrath,[23] V. M. Korablev,[39] A. V. Kozelov,[39] J. Kraus,[65] D. Krop,[54] T. Kuhl,[24] A. Kumar,[69] A. Kupco,[11] T. Kurča,[20] J. Kvita,[9] F. Lacroix,[13] D. Lam,[55] S. Lammers,[70] G. Landsberg,[77] P. Lebrun,[20] W. M. Lee,[50] A. Leflat,[38] J. Lellouch,[17] J. Leveque,[45] J. Li,[78] L. Li,[48] Q. Z. Li,[50] S. M. Lietti,[5] J. G. R. Lima,[52] D. Lincoln,[50] J. Linnemann,[65] V. V. Lipaev,[39] R. Lipton,[50] Y. Liu,[7] Z. Liu,[6] A. Lobodenko,[40] M. Lokajicek,[11] P. Love,[42] H. J. Lubatti,[82] R. Luna,[3] A. L. Lyon,[50] A. K. A. Maciel,[2] D. Mackin,[80] R. J. Madaras,[46] P. Mättig,[26] C. Magass,[21] A. Magerkurth,[64] P. K. Mal,[82] H. B. Malbouisson,[3] S. Malik,[67] V. L. Malyshev,[36] H. S. Mao,[50] Y. Maravin,[59] B. Martin,[14] R. McCarthy,[72] A. Melnitchouk,[66] L. Mendoza,[8] P. G. Mercadante,[5] M. Merkin,[38] K. W. Merritt,[50] A. Meyer,[21] J. Meyer,[22,§] T. Millet,[20] J. Mitrevski,[70] J. Molina,[3] R. K. Mommsen,[44] N. K. Mondal,[29] R. W. Moore,[6] T. Moulik,[58] G. S. Muanza,[20] M. Mulders,[50] M. Mulhearn,[70] O. Mundal,[22] L. Mundim,[3] E. Nagy,[15] M. Naimuddin,[50] M. Narain,[77] N. A. Naumann,[35] H. A. Neal,[64] J. P. Negret,[8] P. Neustroev,[40] H. Nilsen,[23] H. Nogima,[3] S. F. Novaes,[5] T. Nunnemann,[25] V. O'Dell,[50] D. C. O'Neil,[6] G. Obrant,[40] C. Ochando,[16] D. Onoprienko,[59] N. Oshima,[50] N. Osman,[43] J. Osta,[55] R. Otec,[10] G. J. Otero y Garzón,[50] M. Owen,[44] P. Padley,[80] M. Pangilinan,[77] N. Parashar,[56] S.-J. Park,[71] S. K. Park,[31] J. Parsons,[70] R. Partridge,[77] N. Parua,[54] A. Patwa,[73] G. Pawloski,[80] B. Penning,[23] M. Perfilov,[38] K. Peters,[44] Y. Peters,[26] P. Pétroff,[16] M. Petteni,[43] R. Piegaia,[1] J. Piper,[65] M.-A. Pleier,[22] P. L. M. Podesta-Lerma,[33,‡] V. M. Podstavkov,[50] Y. Pogorelov,[55] M.-E. Pol,[2] P. Polozov,[37] B. G. Pope,[65] A. V. Popov,[39] C. Potter,[6] W. L. Prado da Silva,[3] H. B. Prosper,[49] S. Protopopescu,[73] J. Qian,[64] A. Quadt,[22,§] B. Quinn,[66] A. Rakitine,[42]

M. S. Rangel,[2] K. Ranjan,[28] P. N. Ratoff,[42] P. Renkel,[79] S. Reucroft,[63] P. Rich,[44] J. Rieger,[54] M. Rijssenbeek,[72] I. Ripp-Baudot,[19] F. Rizatdinova,[76] S. Robinson,[43] R. F. Rodrigues,[3] M. Rominsky,[75] C. Royon,[18] P. Rubinov,[50] R. Ruchti,[55] G. Safronov,[37] G. Sajot,[14] A. Sánchez-Hernández,[33] M. P. Sanders,[17] A. Santoro,[3] G. Savage,[50] L. Sawyer,[60] T. Scanlon,[43] D. Schaile,[25] R. D. Schamberger,[72] Y. Scheglov,[40] H. Schellman,[53] T. Schliephake,[26] C. Schwanenberger,[44] A. Schwartzman,[68] R. Schwienhorst,[65] J. Sekaric,[49] H. Severini,[75] E. Shabalina,[51] M. Shamim,[59] V. Shary,[18] A. A. Shchukin,[39] R. K. Shivpuri,[28] V. Siccardi,[19] V. Simak,[10] V. Sirotenko,[50] P. Skubic,[75] P. Slattery,[71] D. Smirnov,[55] G. R. Snow,[67] J. Snow,[74] S. Snyder,[73] S. Söldner-Rembold,[44] L. Sonnenschein,[17] A. Sopczak,[42] M. Sosebee,[78] K. Soustruznik,[9] B. Spurlock,[78] J. Stark,[14] J. Steele,[60] V. Stolin,[37] D. A. Stoyanova,[39] J. Strandberg,[64] S. Strandberg,[41] M. A. Strang,[69] E. Strauss,[72] M. Strauss,[75] R. Ströhmer,[25] D. Strom,[53] L. Stutte,[50] S. Sumowidagdo,[49] P. Svoisky,[55] A. Sznajder,[3] P. Tamburello,[45] A. Tanasijczuk,[1] W. Taylor,[6] J. Temple,[45] B. Tiller,[25] F. Tissandier,[13] M. Titov,[18] V. V. Tokmenin,[36] T. Toole,[61] I. Torchiani,[23] T. Trefzger,[24] D. Tsybychev,[72] B. Tuchming,[18] C. Tully,[68] P. M. Tuts,[70] R. Unalan,[65] L. Uvarov,[40] S. Uvarov,[40] S. Uzunyan,[52] B. Vachon,[6] P. J. van den Berg,[34] R. Van Kooten,[54] W. M. van Leeuwen,[34] N. Varelas,[51] E. W. Varnes,[45] I. A. Vasilyev,[39] M. Vaupel,[26] P. Verdier,[20] L. S. Vertogradov,[36] M. Verzocchi,[50] F. Villeneuve-Seguier,[43] P. Vint,[43] P. Vokac,[10] E. Von Toerne,[59] M. Voutilainen,[68,‖] R. Wagner,[68] H. D. Wahl,[49] L. Wang,[61] M. H. L. S. Wang,[50] J. Warchol,[55] G. Watts,[82] M. Wayne,[55] G. Weber,[24] M. Weber,[50] L. Welty-Rieger,[54] A. Wenger,[23,¶] N. Wermes,[22] M. Wetstein,[61] A. White,[78] D. Wicke,[26] G. W. Wilson,[58] S. J. Wimpenny,[48] M. Wobisch,[60] D. R. Wood,[63] T. R. Wyatt,[44] Y. Xie,[77] S. Yacoob,[53] R. Yamada,[50] M. Yan,[61] T. Yasuda,[50] Y. A. Yatsunenko,[36] K. Yip,[73] H. D. Yoo,[77] S. W. Youn,[53] J. Yu,[78] A. Zatserklyaniy,[52] C. Zeitnitz,[26] T. Zhao,[82] B. Zhou,[64] J. Zhu,[72] M. Zielinski,[71] D. Zieminska,[54] A. Zieminski,[54,**] L. Zivkovic,[70] V. Zutshi,[52] and E. G. Zverev[38]

(D0 Collaboration)

[1]*Universidad de Buenos Aires, Buenos Aires, Argentina*
[2]*LAFEX, Centro Brasileiro de Pesquisas Físicas, Rio de Janeiro, Brazil*
[3]*Universidade do Estado do Rio de Janeiro, Rio de Janeiro, Brazil*
[4]*Universidade Federal do ABC, Santo André, Brazil*
[5]*Instituto de Física Teórica, Universidade Estadual Paulista, São Paulo, Brazil*
[6]*University of Alberta, Edmonton, Alberta, Canada;*
Simon Fraser University, Burnaby, British Columbia, Canada;
York University, Toronto, Ontario, Canada;
and McGill University, Montreal, Quebec, Canada
[7]*University of Science and Technology of China, Hefei, People's Republic of China*
[8]*Universidad de los Andes, Bogotá, Colombia*
[9]*Center for Particle Physics, Charles University, Prague, Czech Republic*
[10]*Czech Technical University, Prague, Czech Republic*
[11]*Center for Particle Physics, Institute of Physics, Academy of Sciences of the Czech Republic, Prague, Czech Republic*
[12]*Universidad San Francisco de Quito, Quito, Ecuador*
[13]*LPC, Université Blaise Pascal, CNRS/IN2P3, Clermont, France*
[14]*LPSC, Université Joseph Fourier Grenoble 1, CNRS/IN2P3, Institut National Polytechnique de Grenoble, France*
[15]*CPPM, IN2P3/CNRS, Université de la Méditerranée, Marseille, France*
[16]*LAL, Université Paris-Sud, IN2P3/CNRS, Orsay, France*
[17]*LPNHE, IN2P3/CNRS, Universités Paris VI and VII, Paris, France*
[18]*DAPNIA/Service de Physique des Particules, CEA, Saclay, France*
[19]*IPHC, Université Louis Pasteur et Université de Haute Alsace, CNRS/IN2P3, Strasbourg, France*
[20]*IPNL, Université Lyon 1, CNRS/IN2P3, Villeurbanne, France, and Université de Lyon, Lyon, France*
[21]*III. Physikalisches Institut A, RWTH Aachen, Aachen, Germany*
[22]*Physikalisches Institut, Universität Bonn, Bonn, Germany*
[23]*Physikalisches Institut, Universität Freiburg, Freiburg, Germany*
[24]*Institut für Physik, Universität Mainz, Mainz, Germany*
[25]*Ludwig-Maximilians-Universität München, München, Germany*
[26]*Fachbereich Physik, University of Wuppertal, Wuppertal, Germany*
[27]*Panjab University, Chandigarh, India*
[28]*Delhi University, Delhi, India*
[29]*Tata Institute of Fundamental Research, Mumbai, India*
[30]*University College Dublin, Dublin, Ireland*
[31]*Korea Detector Laboratory, Korea University, Seoul, Korea*
[32]*SungKyunKwan University, Suwon, Korea*

[33]CINVESTAV, Mexico City, Mexico
[34]FOM-Institute NIKHEF and University of Amsterdam/NIKHEF, Amsterdam, The Netherlands
[35]Radboud University Nijmegen/NIKHEF, Nijmegen, The Netherlands
[36]Joint Institute for Nuclear Research, Dubna, Russia
[37]Institute for Theoretical and Experimental Physics, Moscow, Russia
[38]Moscow State University, Moscow, Russia
[39]Institute for High Energy Physics, Protvino, Russia
[40]Petersburg Nuclear Physics Institute, St. Petersburg, Russia
[41]Lund University, Lund, Sweden; Royal Institute of Technology and Stockholm University, Stockholm, Sweden; and Uppsala University, Uppsala, Sweden
[42]Lancaster University, Lancaster, United Kingdom
[43]Imperial College, London, United Kingdom
[44]University of Manchester, Manchester, United Kingdom
[45]University of Arizona, Tucson, Arizona 85721, USA
[46]Lawrence Berkeley National Laboratory and University of California, Berkeley, California 94720, USA
[47]California State University, Fresno, California 93740, USA
[48]University of California, Riverside, California 92521, USA
[49]Florida State University, Tallahassee, Florida 32306, USA
[50]Fermi National Accelerator Laboratory, Batavia, Illinois 60510, USA
[51]University of Illinois at Chicago, Chicago, Illinois 60607, USA
[52]Northern Illinois University, DeKalb, Illinois 60115, USA
[53]Northwestern University, Evanston, Illinois 60208, USA
[54]Indiana University, Bloomington, Indiana 47405, USA
[55]University of Notre Dame, Notre Dame, Indiana 46556, USA
[56]Purdue University Calumet, Hammond, Indiana 46323, USA
[57]Iowa State University, Ames, Iowa 50011, USA
[58]University of Kansas, Lawrence, Kansas 66045, USA
[59]Kansas State University, Manhattan, Kansas 66506, USA
[60]Louisiana Tech University, Ruston, Louisiana 71272, USA
[61]University of Maryland, College Park, Maryland 20742, USA
[62]Boston University, Boston, Massachusetts 02215, USA
[63]Northeastern University, Boston, Massachusetts 02115, USA
[64]University of Michigan, Ann Arbor, Michigan 48109, USA
[65]Michigan State University, East Lansing, Michigan 48824, USA
[66]University of Mississippi, University, Mississippi 38677, USA
[67]University of Nebraska, Lincoln, Nebraska 68588, USA
[68]Princeton University, Princeton, New Jersey 08544, USA
[69]State University of New York, Buffalo, New York 14260, USA
[70]Columbia University, New York, New York 10027, USA
[71]University of Rochester, Rochester, New York 14627, USA
[72]State University of New York, Stony Brook, New York 11794, USA
[73]Brookhaven National Laboratory, Upton, New York 11973, USA
[74]Langston University, Langston, Oklahoma 73050, USA
[75]University of Oklahoma, Norman, Oklahoma 73019, USA
[76]Oklahoma State University, Stillwater, Oklahoma 74078, USA
[77]Brown University, Providence, Rhode Island 02912, USA
[78]University of Texas, Arlington, Texas 76019, USA
[79]Southern Methodist University, Dallas, Texas 75275, USA
[80]Rice University, Houston, Texas 77005, USA
[81]University of Virginia, Charlottesville, Virginia 22901, USA
[82]University of Washington, Seattle, Washington 98195, USA

(Received 19 March 2008; published 15 May 2008)

We measure the $t\bar{t}$ production cross section in $p\bar{p}$ collisions at $\sqrt{s} = 1.96$ TeV in the lepton + jets channel. Two complementary methods discriminate between signal and background: b tagging and a kinematic likelihood discriminant. Based on 0.9 fb^{-1} of data collected by the D0 detector at the Fermilab Tevatron Collider, we measure $\sigma_{t\bar{t}} = 7.62 \pm 0.85$ pb, assuming the current world average $m_t = 172.6$ GeV. We compare our cross section measurement with theory predictions to determine a value for the top-quark mass of 170 ± 7 GeV.

DOI: 10.1103/PhysRevLett.100.192004 PACS numbers: 13.85.Lg, 13.85.Qk, 14.65.Ha

The standard model fixes all properties of the top quark except its mass. The top-quark production cross section depends on the couplings of the top quark and on its mass. For a top-quark mass of 175 GeV, the standard model predicts a top-quark–top-antiquark pair ($t\bar{t}$) production cross section of about 6.7 pb [1,2] at the Tevatron, which collides protons and antiprotons at $\sqrt{s} = 1.96$ TeV. Previous measurements [3,4] agree with this prediction within their precision of 15%. In this Letter, we report the most precise measurement of the $t\bar{t}$ production cross section to date, based on data collected by the D0 detector [5] between August 2002 and December 2005 with an integrated luminosity of 0.9 fb^{-1}. We compare the measured cross section to predictions to test whether the top quark conforms with standard model expectations and for the first time extract a constraint on the top-quark mass based only on this comparison. This provides a top-quark mass measurement in a well-defined renormalization scheme, that employed in the cross section calculation, that is complementary to direct measurements.

In the standard model, the top quark nearly always decays to a W boson and a b quark. The decay modes of the W boson define the possible final states. Here we focus on the lepton + jets channel in which one W boson decays to $e\nu$, $\mu\nu$, or $\tau\nu$ followed by $\tau \to e\nu\bar{\nu}$ or $\mu\nu\bar{\nu}$. We refer to such leptons as prompt. The other W boson decays to jets or to $\tau\nu$ followed by a hadronic τ decay. The branching fraction for this channel is 38%.

The D0 detector acquires these events by triggering on an electron or muon and at least one jet with a large momentum component transverse to the beam direction (p_T). The event selection [6] requires exactly one electron or muon, isolated from other objects in the detector, with $p_T > 20$ GeV and $|\eta| < 1.1$ (for e) or $|\eta| < 2$ (for μ), missing transverse momentum $\not{p}_T > 20$ (for e + jets) or 25 GeV (for μ + jets), and at least three jets with $p_T > 20$ GeV and $|\eta| < 2.5$. The pseudorapidity is defined as $\eta = -\ln[\tan(\theta/2)]$, and θ is the polar angle with the proton beam. The leading jet must have $p_T > 40$ GeV, and the lepton p_T and $\not{p}_T$ vectors must be separated in azimuth to reject background events with mismeasured particles. Jets are reconstructed by using the run II cone algorithm [7] with cone size 0.5. We call this the inclusive lepton + jets sample. Table I gives the number of selected events (N_{data}). The $t\bar{t}$ signal accounts only for about 20% of this sample. Most events originate from other processes that produce prompt leptons and jets (mostly W + jets production) and from events with jets which mimic the signature of a lepton. We use two complementary techniques to distinguish the $t\bar{t}$ signal from these backgrounds: b tagging and a kinematic likelihood discriminant.

We model the $t\bar{t}$ signal and all backgrounds with prompt leptons by using Monte Carlo (MC) simulations. We carry out the analyses by using $t\bar{t}$ events generated at a reference mass of 175 GeV. W + jets and Z + jets production are generated by using the ALPGEN [8] generator and PYTHIA [9] for showering. A matching algorithm [10] avoids double counting of final states. Single top production is generated by using SINGLETOP [11] and COMPHEP [12]. Diboson and $t\bar{t}$ production are generated by PYTHIA. All simulated events are processed by a detector simulation based on GEANT [13] and by the same reconstruction programs as the collider data.

We first determine the background from events without prompt leptons in the inclusive lepton + jets sample by using loose data samples defined by relaxing the electron identification and the muon isolation requirements. We use simulated events to determine the probability ϵ_s for leptons from W boson decays that satisfy the loose selection to also pass the selection used for the measurement. We correct this efficiency for differences between MC simulation and data. We determine the corresponding efficiency ϵ_b for misidentified leptons by using data selected with the criteria given above except for requiring $\not{p}_T < 10$ GeV to minimize contributions from leptons from W boson decays. The number of events in our selected sample is $N_{\text{data}} = N_{\ell\text{j}} + N_{\text{jj}}$, where $N_{\ell\text{j}}$ is the number of events with prompt leptons and N_{jj} the number of events without prompt leptons. The number of events in the corresponding loose sample is $N_{\text{loose}} = N_{\ell\text{j}}/\epsilon_s + N_{\text{jj}}/\epsilon_b$. These two equations determine N_{jj} given in Table I. We predict the number of events N_{other} from the smaller background processes (single top, Z + jets, and diboson production) by using the MC simulation and next-to-leading order cross sections [14].

For the b-tag analysis, we start with the expected $t\bar{t}$ cross section to get a first estimate of the number of $t\bar{t}$ events in the sample. After we obtain a cross section as described below, we update this estimate by using the measured cross section and iterate the cross section calculation until the result is stable. We fix the number of W + jets events in the inclusive sample so that the sum of all background and signal contributions equals the observed number of events.

The b-tag analysis requires that at least one jet be tagged as a b jet, i.e., identified to contain the decay of a long-lived particle such as a b hadron [15]. We determine the number of background events without prompt leptons as above and the number of events expected from other background

TABLE I. Event counts in the inclusive lepton + jets sample.

	e + 3 jets	$e+ \geq 4$ jets	μ + 3 jets	$\mu+ \geq 4$ jets
N_{data}	1300	320	1120	306
N_{loose}	2592	618	1389	388
ϵ_s (%)	84.8 ± 0.3	84.0 ± 1.8	87.3 ± 0.5	84.5 ± 2.2
ϵ_b (%)	19.5 ± 1.7	19.5 ± 1.7	27.2 ± 5.4	27.2 ± 5.4
$N_{t\bar{t}}$	182 ± 20	156 ± 17	137 ± 15	129 ± 14
$N_{W\text{jets}}$	718 ± 42	69 ± 20	802 ± 26	131 ± 16
N_{other}	132 ± 15	35 ± 4	139 ± 15	36 ± 4
N_{jj}	268 ± 34	60 ± 10	42 ± 14	10 ± 6

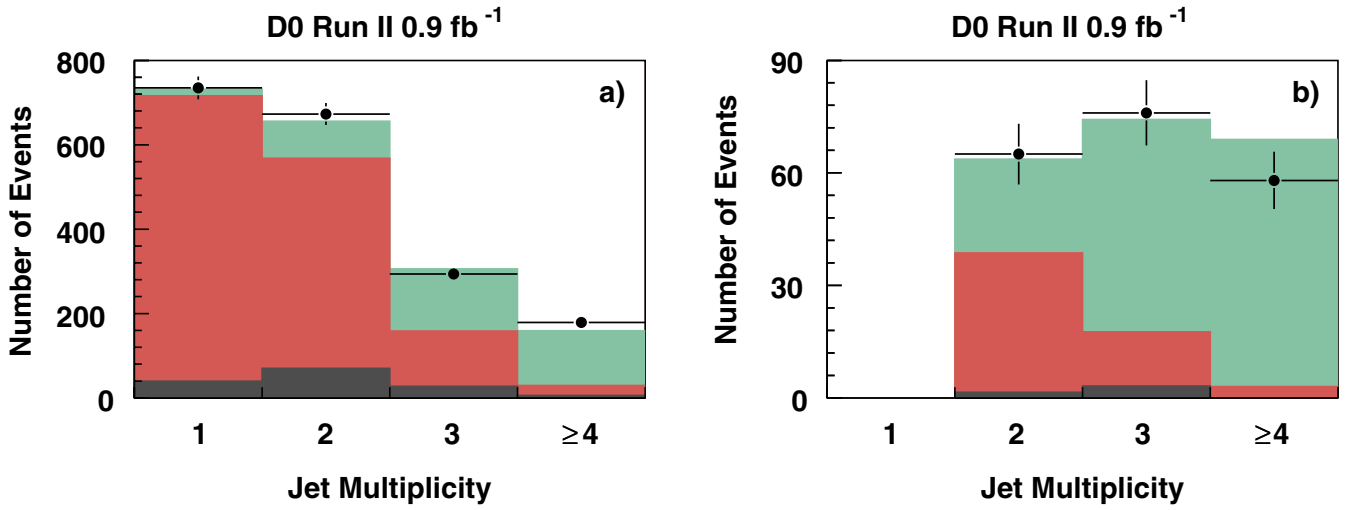

FIG. 1 (color online). Jet multiplicity spectra for e + jets and μ + jets events (a) with one b-tagged jet and (b) with at least two b-tagged jets. The histograms show (from top to bottom) the contributions from $t\bar{t}$ production and from backgrounds with prompt leptons and without prompt leptons.

sources from the number of background events in the inclusive sample times their probability to be b tagged. We obtain the b tagging probability from the MC simulation corrected for differences in the b tagging efficiencies observed in the simulation and in data. We scale the fraction of W + jets events with heavy quarks (b, c) by a factor determined so that the MC model correctly predicts the number of events with two jets and at least one b-tagged jet. Figure 1 shows the jet multiplicity spectrum of events with b tags compared to expectations. The composition of the b-tagged samples is given in Table II. The $t\bar{t}$ contribution in Fig. 1 and Tables I and II is based on the cross section measured in the b-tag analysis.

We calculate the cross section by using a maximum likelihood fit [16] to the number of events in eight different channels defined by lepton flavor (e, μ), jet multiplicity (3, $\geq$ 4), and b-tag multiplicity (1, $\geq$ 2). The likelihood is defined as $\mathcal{L} = \prod_i \mathcal{P}(N_i, \mu_i(\sigma_{t\bar{t}}))$, where i runs over the eight channels and $\mathcal{P}(N, \mu)$ is the Poisson probability to observe N events when μ are expected. The expected number of events is the sum of the number of events from all backgrounds plus the number of $t\bar{t}$ events as a function of $\sigma_{t\bar{t}}$. We obtain $\sigma_{t\bar{t}} = 8.05 \pm 0.54(\text{stat}) \pm 0.70(\text{syst}) \pm 0.49(\text{lumi})$ pb for $m_t = 175$ GeV. The third uncertainty arises from the measurement of the integrated luminosity [17].

Table III lists the systematic uncertainties from the following categories. Selection covers acceptance and efficiency for leptons and jets. Jet energy calibration accounts for jet energy scale and resolution. The b tagging efficiencies for b, c, and light quark or gluon jets make up the b-tagging uncertainty. MC model uncertainties originate from the cross sections used to normalize the simulated backgrounds, differences observed between $t\bar{t}$ samples generated with ALPGEN and PYTHIA, the factorization and renormalization scale in the W + jets simulation, and the parton distribution functions (PDFs). N_{jj} covers the determination of the number of events without prompt leptons.

The likelihood analysis is based on kinematic differences between events with $t\bar{t}$ decays and backgrounds. We build a likelihood discriminant from 5–6 variables, listed in Table IV, in each channel. The variables were selected to be well modeled by the MC simulation and to have good discrimination power. For this analysis, we use the inclusive lepton + jets sample with the additional re-

TABLE II. Numbers of events in the b-tagged analysis. $N_{t\bar{t}}$ is based on the cross section measured by the b-tag analysis.

	3 jets, 1 tag	3 jets, $\geq$ 2 tags	$\geq$ 4 jets, 1 tag	$\geq$ 4 jets, $\geq$ 2 tags
$N_{t\bar{t}}$	147 ± 12	57 ± 6	130 ± 10	66 ± 7
$N_{W\text{jets}}$	105 ± 5	10 ± 1	16 ± 2	2 ± 1
N_{other}	27 ± 2	5 ± 1	8 ± 1	2 ± 1
N_{jj}	27 ± 6	3 ± 2	6 ± 3	0 ± 2
Total	306 ± 14	74 ± 6	159 ± 11	69 ± 7
N_{data}	294	76	179	58

TABLE III. Breakdown of systematic uncertainties.

Source	b-tag	Likelihood	Combined
Selection efficiency	0.26 pb	0.25 pb	0.25 pb
Jet energy calibration	0.30 pb	0.11 pb	0.20 pb
b tagging	0.48 pb	-	0.24 pb
MC model	0.29 pb	0.11 pb	0.19 pb
N_{jj}	0.06 pb	0.10 pb	0.07 pb
Likelihood fit	-	0.15 pb	0.08 pb

TABLE IV. Variables used for the likelihood discriminant. $\Delta R = \sqrt{(\Delta\phi)^2 + (\Delta\eta)^2}$ and i indexes the list of N_j jets with $p_T > 15$ GeV, ordered in decreasing p_T.

Variable	Channel
$\sum_{i=3}^{N_j} p_T(i)$	All
$\sum_{i=1}^{N_j} p_T(i) / \sum_{i=1}^{N_j} p_z(i)$	e + 3 jets, $e+ \geq 4$ jets
$\sum_{i=1}^{N_j} p_T(i) + p_T(e) + \not{p}_T$	e + 3 jets, $e+ \geq 4$ jets
ΔR between lepton and jet 1	All
ΔR between jets 1 and 2	$e+ \geq 4$ jets, $\mu+ \geq 4$ jets
$\Delta\phi$ between lepton and $\not{p}_T$	μ + 3 jets, $\mu+ \geq 4$ jets
$\Delta\phi$ between jet 1 and $\not{p}_T$	e + 3 jets, μ + 3 jets
Sphericity	All but μ + 3 jets
Aplanarity	All but μ + 3 jets

quirement that events with three jets must satisfy $\sum_{i=1}^{N_j} p_T(i) > 120$ GeV. The events are divided into four channels defined by lepton flavor and jet multiplicity (3, ≥ 4).

We determine the probability density functions of the likelihood discriminant for signal and prompt lepton backgrounds from the simulation and for events without prompt leptons from a control data sample. We perform a maximum likelihood fit to the likelihood discriminant distributions from data in all four channels simultaneously with the $t\bar{t}$ production cross section as a free parameter. The number of events without prompt leptons is constrained to the value obtained from the loose data sample in the same way as described above. Table V gives the sample composition for the best fit, and Fig. 2 shows the corresponding likelihood discriminant distributions. We measure $\sigma_{t\bar{t}} = 6.62 \pm 0.78(\text{stat}) \pm 0.36(\text{syst}) \pm 0.40(\text{lumi})$ pb for $m_t = 175$ GeV. The systematic uncertainties are listed in Table III in the same categories as for the b-tag analysis plus the likelihood fit uncertainty from statistical fluctuations in the likelihood discriminant shapes.

TABLE V. Sample composition from the likelihood fit. $N_{t\bar{t}}$ is based on the cross section measured by the likelihood analysis.

	3 jets	≥ 4 jets
N_{data}	1760	626
$N_{t\bar{t}}$	245 ± 20	233 ± 19
$N_{W\text{jets}} + N_{\text{other}}$	1294 ± 48	321 ± 30
N_{jj}	227 ± 28	70 ± 12

We combine the two analyses by using the best linear unbiased estimate method [18]. Their statistical correlation factor is 0.31, determined by MC generated pseudodata sets. The systematic uncertainties from each source are completely correlated between both analyses. The combined result is $\sigma_{t\bar{t}} = 7.42 \pm 0.53(\text{stat}) \pm 0.46(\text{syst}) \pm 0.45(\text{lumi})$ pb for $m_t = 175$ GeV with $\chi^2 = 2$, corresponding to a p value of 0.16. We use $t\bar{t}$ events simulated with different values of the top-quark mass to determine the cross section as a function of top-quark mass. A polynomial fit gives $\sigma_{t\bar{t}}/\text{pb} = 7.42 - 7.9 \times 10^{-2}\Delta m + 9.7 \times 10^{-4}(\Delta m)^2 - 1.7 \times 10^{-5}(\Delta m)^3$, where $\Delta m = m_t/\text{GeV} - 175$, as shown in Fig. 3.

We define likelihoods as a function of $\sigma_{t\bar{t}}$ and m_t for the theory prediction and our measurement. For each value of m_t, we represent the theory uncertainty from the termination of the perturbative calculation by a likelihood function that is constant within the ranges given in Refs. [1,2] and zero elsewhere and the PDF uncertainty by a Gaussian likelihood function with rms equal to the uncertainty determined in Ref. [1] for the CTEQ6M [19] error PDF sets. We then convolute the two functions and average the like-

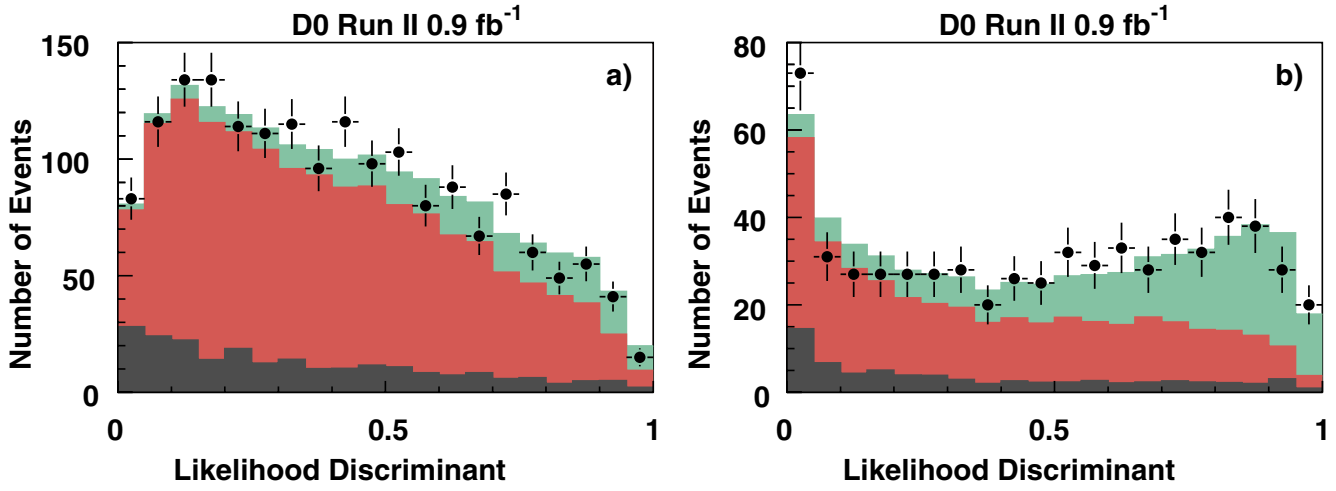

FIG. 2 (color online). Likelihood discriminant distributions for e + jets and μ + jets events (a) with 3 jets and (b) with at least 4 jets. The histograms show (from top to bottom) the contributions from $t\bar{t}$ production and from backgrounds with prompt leptons and without prompt leptons.

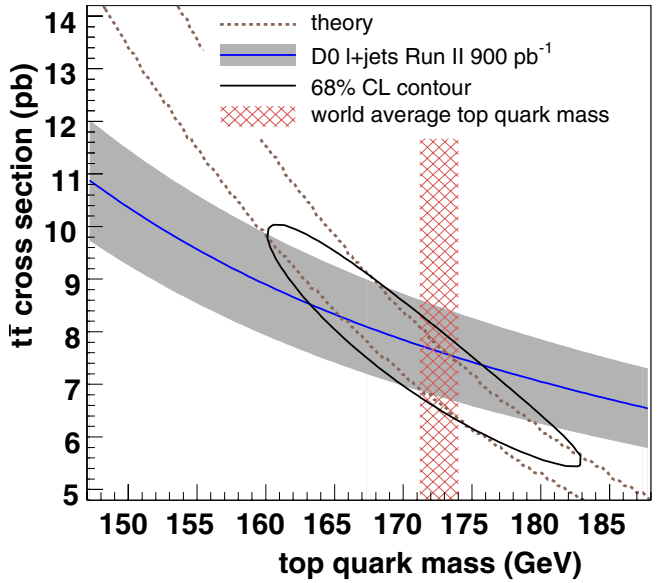

FIG. 3 (color online). Comparison of measured cross section and theory prediction versus top-quark mass.

lihood functions from the two calculations. The cross section measurement is represented by a Gaussian likelihood function centered on the measured value with rms equal to the total experimental uncertainty. We multiply the theory and measurement likelihoods to obtain a joint likelihood. The contour in Fig. 3 shows the smallest region of the joint likelihood that contains 68% of its integral. We integrate over the cross section to get a likelihood function that depends only on the top-quark mass and find $m_t = 170 \pm 7$ GeV at 68% C.L., in agreement with the world average of direct measurements of the top-quark mass of 172.6 ± 1.4 GeV [20].

In conclusion, we find that $t\bar{t}$ production in $p\bar{p}$ collisions agrees with standard model predictions. At the world average top-quark mass of 172.6 GeV, we measure $\sigma_{t\bar{t}} = 7.62 \pm 0.85$ pb. This is the most precise measurement of the $t\bar{t}$ production cross section. By comparing this measurement with the theory prediction, we determine the top-quark mass to be 170 ± 7 GeV.

We thank the staffs at Fermilab and collaborating institutions and acknowledge support from the DOE and NSF (USA); CEA and CNRS/IN2P3 (France); FASI, Rosatom, and RFBR (Russia); CNPq, FAPERJ, FAPESP, and FUNDUNESP (Brazil); DAE and DST (India); Colciencias (Colombia); CONACyT (Mexico); KRF and KOSEF (Korea); CONICET and UBACyT (Argentina); FOM (The Netherlands); STFC (United Kingdom); MSMT and GACR (Czech Republic); CRC Program, CFI, NSERC, and WestGrid Project (Canada); BMBF and DFG (Germany); SFI (Ireland); The Swedish Research Council (Sweden); CAS and CNSF (China); and the Alexander von Humboldt Foundation.

*Visiting scientist from Augustana College, Sioux Falls, SD, USA.
†Visiting scientist from The University of Liverpool, Liverpool, United Kingdom.
‡Visiting scientist from ICN-UNAM, Mexico City, Mexico.
§Visiting scientist from II. Physikalisches Institut, Georg-August-University, Göttingen, Germany.
‖Visiting scientist from Helsinki Institute of Physics, Helsinki, Finland.
¶Visiting scientist from Universität Zürich, Zürich, Switzerland.
**Deceased.

[1] M. Cacciari *et al.*, J. High Energy Phys. 04 (2004) 068.
[2] N. Kidonakis and R. Vogt, Phys. Rev. D **68**, 114014 (2003).
[3] V. M. Abazov *et al.* (D0 Collaboration), Phys. Rev. D **74**, 112004 (2006); **76**, 052006 (2007).
[4] A. Abulencia *et al.* (CDF Collaboration), Phys. Rev. Lett. **97**, 082004 (2006).
[5] V. M. Abazov *et al.* (D0 Collaboration), Nucl. Instrum. Methods Phys. Res., Sect. A **565**, 463 (2006).
[6] V. M. Abazov *et al.* (D0 Collaboration), Phys. Rev. D **76**, 092007 (2007).
[7] G. Blazey *et al.*, arXiv:hep-ex/0005012.
[8] M. L. Mangano *et al.*, J. High Energy Phys. 07 (2003) 001.
[9] T. Sjöstrand *et al.*, arXiv:hep-ph/0308153.
[10] S. Höche *et al.*, arXiv:hep-ph/0602031.
[11] E. E. Boos *et al.*, Phys. At. Nucl. **69**, 1317 (2006).
[12] E. E. Boos *et al.* (CompHEP Collaboration), Nucl. Instrum. Methods Phys. Res., Sect. A **534**, 250 (2004).
[13] R. Brun and F. Carminati, CERN Program Library Long Writeup No. W5013, 1993.
[14] E. E. Boos *et al.*, Phys. At. Nucl. **69**, 1317 (2006); Z. Sullivan, Phys. Rev. D **70**, 114012 (2004); J. M. Campbell and R. K. Ellis, Phys. Rev. D **60**, 113006 (1999).
[15] T. Scanlon, Ph.D. thesis [Fermilab Report No. FERMILAB-THESIS-2006-43].
[16] V. M. Abazov *et al.* (D0 Collaboration), Phys. Rev. D **74**, 112004 (2006).
[17] T. Andeen *et al.*, Report No. FERMILAB-TM-2365, 2007.
[18] L. Lyons, D. Gibaut, and P. Clifford, Nucl. Instrum. Methods Phys. Res., Sect. A **270**, 110 (1988); A. Valassi, Nucl. Instrum. Methods Phys. Res., Sect. A **500**, 391 (2003).
[19] D. Stump *et al.*, J. High Energy Phys. 10 (2003) 046.
[20] CDF and D0 Collaborations, Report No. FERMILAB-TM-2403-E.